Arabian Journal of Chemistry (2019) **12**, 1463–1473

King Saud University

Arabian Journal of Chemistry

www.ksu.edu.sa
www.sciencedirect.com

ORIGINAL ARTICLE

Synthesis, spectral, crystal structural, antimicrobial, DNA interaction and thermal behavior of some new zinc halide complexes: 3D supramolecular structure of zinc bromide complex

M. Montazerozohori [a,*], S.A. Musavi [a], A. Masoudi-asl [a], H. Mohammadi [a], R. Naghiha [b], A. Assoud [c]

[a] *Department of Chemistry, Yasouj University, Yasouj 7591874831, Iran*
[b] *Department of Animal Science, Yasouj University, Yasouj 7591874831, Iran*
[c] *Department of Chemistry, University of Waterloo, Waterloo, Ontario N2L 3G1, Canada*

Received 20 August 2014; accepted 3 November 2014
Available online 13 November 2014

KEYWORDS

Schiff base;
Zn(II);
DNA cleavage;
TG/DTG analysis;
X-ray;
Tetrahedral

Abstract Three new four coordinated zinc(II) complexes have been synthesized and characterized by IR, UV, elemental analysis, ^{1}H and ^{13}C NMR and X-ray single crystal analysis. The elemental analyses of the complexes are in agreement with the general formula of $ZnLX_2$ wherein L = Schiff base ligand and X = Cl^-, Br^- and I^-. Low molar conductivities in DMF indicated non-electrolyte character of all complexes. Spectroscopic studies well confirmed the coordination via azomethine nitrogens of the ligand to zinc ion. The single crystal X-ray analysis shows that $ZnLBr_2$ crystallizes in the triclinic crystal system with space group $P\bar{1}$. It contains two crystallographically independent molecules noted as A and B, with both Zn1A and Zn1B being almost in perfect tetrahedral environments (τ_4 = 0.94 for Zn1A and τ_4 = 0.93 for Zn1B). A detailed structural analysis shows that there are three non-classical hydrogen bondings of C–H. . .Br in the structure. Various C–H. . .π and C–H. . .Br interactions play an important role in stabilizing the molecular structure and then give rise to a 3D supramolecular structure of the $ZnLBr_2$ complex. After characterization, the Schiff base and its complexes were screened *in vitro* for their antibacterial and antifungal activities by disk diffusion technique. Also the ability of the complexes for DNA cleavage was studied by agarose gel

* Corresponding author. Tel./fax: +98 74133223048.
E-mail address: mmzohory@yahoo.com (M. Montazerozohori).
Peer review under responsibility of King Saud University.

Production and hosting by Elsevier

http://dx.doi.org/10.1016/j.arabjc.2014.11.005

electrophoresis method. Finally, thermal behavior of the complexes has been studied by thermogravimetry and then some activation kinetics parameters of decomposition steps were evaluated based on TG/DTG plots.

1. Introduction

Medicinal properties of coordination compounds derived from zinc metal ion and Schiff base ligands have been widely investigated, including different areas of medicinal chemistry. The Zn(II) complex of a tridentate Schiff base ligand derived from 2-acetylpyridine and l-tryptophan was found to be anticancer (Zhang et al., 2012). Zinc(II) complexes of the 2-{[2-(2-hydroxyethylamino)ethylimino]methyl}-4-nitrophenol ligand have been shown to possess urease inhibitory activities (You et al., 2010). The bidentate Schiff base ligand of 5-methylthiophene-2-carboxaldehyde-carbohydrazone and its zinc complexes has been used as antioxidant (Harinath et al., 2013). The Zn(II) complex of naphthofuran-2-carbohydrazide Schiff base efficiently cleaves DNA in comparison to other metal complexes (Halli and Sumathi, 2012). Cu(II)/Zn(II) complexes of the chiral heterocyclic Schiff base showed good binding with CT-DNA and mononucleotides (Arjmand et al., 2011). Schiff base derived from 5-bromosalicylaldehyde and 2-aminomethylthiophene and its metal complexes were found to be antibacterial and cytotoxically active (El-Sherif and Eldebss, 2011). Zn(II) complexes of a bidentate Schiff base derived from isatin and 2-aminopyrimidine showed superoxidase dismutase and antimicrobial activity (Nitha et al., 2014; Abdel Aziz et al., 2012). Results of these studies are promising in most cases and also indicate that the binding of metal to ligand strongly reinforces biological activity (Rosu et al., 2010; Kowol et al., 2010). These reported studies have encouraged us to develop our studies on the biological activity of Schiff base ligands and their complexes. In continuation of our previous works (Montazerozohori et al., 2013, 2014a,b,c) herein we report the synthesis and characterization of new Zn(II) Schiff base complexes formulated as $ZnLX_2$. All compounds were identified by molar conductivity, FT-IR, UV–Vis, ^1H and ^{13}C NMR. The structure of the zinc bromide complex was confirmed by single-crystal X-ray analysis and the results showed that the coordination geometry around the metal ions is slightly distorted tetrahedral. Furthermore, antimicrobial activities, DNA cleavage abilities and thermal behavior (TG/DTG/DTA) of all complexes were investigated.

2. Experimental

2.1. Materials and methods

All solvents used in the synthesis and analysis, 3-phenyl-propenal, 2,2-dimethyl-propane-1,3-diamine, zinc salts and other chemicals were purchased from Aldrich and Merck, and used without further purification. The FT-IR spectra were recorded on the JASCO-680 model in the range of 400–4000 cm^{-1} using KBr disks. Elemental analysis (C, N and H) was conducted on a CHNS-932(leco) elemental analyzer. UV–Vis spectra were recorded in the 200–800 nm range using a JASCO-V570 spectrometer at DMF. ^1H and ^{13}C NMR spectra were recorded by a Brucker DPX FT-NMR spectrometer at 400 MHz in $CDCl_3$ using TMS as internal standard. Molar conductance of the Schiff base ligand and their zinc complexes were determined in DMF (1.0×10^{-3} M) at room temperature by a Metrohm 712 conductometer. The melting or decomposition temperatures (°C) of the complexes were recorded on the Kruss instrument. In biological tests, Nutrient agar (Merck, Germany) was used as the solid medium for preparing nutrient plates, while Mueller Hinton broth (Scharlab) was used as the liquid culture media. *Escherichia coli* ATCC 25922, *Pseudomonas aeruginosa* ATCC 9027, *Staphylococcus aureus* ATCC 6538 and *Bacillus subtilis* ATCC 6633 were selected for antibacterial studies and *Candida albicans* was a candidate for antifungal test. Thermal behaviors were investigated by Diamond TGA PerkinElmer.

2.2. Synthesis of Schiff base ligand (L)

The Schiff base ligand was synthesized according to the previous report via a condensation reaction between 2,2-dimethyl-propane-1,3-diamine and 3-phenyl-2-propenal (Joohari, 2013). Ligand was filtered and washed twice with cooled ethanol and recrystallized from ethanol–dichloromethane solvent mixture.

2.3. Synthesis of complexes

Zinc complexes were prepared by addition of an ethanolic solution of the Schiff base (1 mmol, 0.3305 g) to the corresponding zinc salt solution (1 mmol in ethanol) under vigorous stirring at room temperature. The zinc complex precipitate was filtered, then washed with cooled ethanol and dried under vacuum. Crystals of $ZnLBr_2$ suitable for X-ray analysis were obtained by slow evaporation from acetonitrile as solvent at room temperature. Physical and spectral data of ligand and its zinc complexes have been collected in Tables 1–3.

2.4. Single-crystal X-ray diffraction

Suitable single crystal for structure determination was selected and mounted on glass fibers using a Bruker Kappa Apex II CCD diffractometer with graphite-monochromatized Mo-$K\alpha$ radiation (λ = 0.71073 Å). Data were collected at room temperature by scanning ω and ϕ in set of blocks, with exposure times of 20 s. Data were corrected for Lorentz and polarization effects. Absorption corrections were based on fitting a function to the empirical transmission surface as sampled by multiple equivalent measurements using the *SADABS* part of the *APEX II* package since there were no clear faces for indexation. The structure was solved using direct methods and

Table 1 Analytical and physical data of the Schiff base ligand (L) and its Zn(II) complexes.

	Compound	Molecular formula	Color	Melting point	Yield (%)	Found (Calcd.) (%)			ΛM ($cm^2\ \Omega^{-1}\ M^{-1}$)
						C	N	H	
1	Ligand(L)	$C_{23}H_{26}N_2$	Orange	93	65	83.4(83.59)	8.8(8.48)	7.5(7.93)	6.68
2	$ZnLCl_2$	$C_{23}H_{26}Cl_2ZnN_2$	White	247	87	59.1(59.18)	6.2(6.00)	5.5(5.61)	13.50
3	$ZnLBr_2$	$C_{23}H_{26}Br_2ZnN_2$	White	240	84	49.9(49.71)	5.3(5.04)	4.6(4.72)	11.00
4	$ZnLI_2$	$C_{23}H_{26}I_2ZnN_2$	White	210	78	42.1(42.52)	4.3(4.31)	4.2(4.03)	49.90

Table 2 Vibrational (cm^{-1}) and electronic (nm) spectral data of the Schiff base (L) and its complexes.

	Compound	νCH_{arom}	νCH_{alkene}	$\nu CH_{aliph.}$	νCH_{imin}	νC=N	νC=C	$\nu CH_{arom(oop)}$	$\nu C–C_{arom(oop)}$	νM–N	λ_{max}
1	L	3058	3025	2954, 2924	2866, 2830	1635	1577	748	690	–	278
2	$ZnLCl_2$	3055	3026	2959, 2922	2871	1629	1606	749	689	443	286
3	$ZnLBr_2$	3055	3019	2957, 2920	2869	1630	1605	748	688	445	286
4	$ZnLI_2$	3054	3022	2959, 2922	2867	1626	1592	750	687	443	286

Table 3 ^1H NMR and ^{13}C NMR chemical shifts of ligand and its Zn (II) complexes in ppm.

Compounds	Proposed assignment of protons and carbons	
L	^1H NMR	8.08(d, $2H_f$, J = 7.20 Hz), 7.44(bd, $4H_{c,c'}$), 7.37(bm, $6H_{b,b',a}$), 7.31(bd, $2H_e$), 6.93(bd, $2H_d$), 3.71(q, $4H_g$), 1.24(t, $6H_h$)
	^{13}C NMR	173.01, 163.72, 138.07, 128.82, 128.53, 127.26, 126.42, 58.22, 46.25, 18.46
$ZnLCl_2$	^1H NMR	8.21(dd, $2H_e$, J = 15.43 & J = 9.76 Hz), 8.02(d, $2H_f$, J = 9.76 Hz), 7.64(dd, $4H_{c,c'}$, J = 6.90 & J = 3.39 Hz), 7.41(t, $6H_{b,b',a}$, J = 3.60 & J = 2.40 Hz), 7.20(d, $2H_d$, J = 15.60 Hz), 3.78(s, $4H_g$), 0.99(s, $6H_h$)
	^{13}C NMR	170.93, 150.10, 134.46, 131.03, 129.05, 128.69, 124.23, 71.84, 36.91, 24.53
$ZnLBr_2$	^1H NMR	8.26(dd, $2H_e$, J = 15.60 & J = 9.60 Hz), 8.07(d, $2H_f$, J = 10.00 Hz), 7.70(m, $4H_{c,c'}$), 7.42(m, $6H_{b,b',a}$), 7.22(d, $2H_d$, J = 15.60 Hz), 3.75(s, $4H_g$), 1.03(s, $6H_h$)
	^{13}C NMR	170.93, 150.22, 134.47, 131.09, 129.07, 128.73, 124.23, 71.25, 36.80, 24.67
$ZnLI_2$	^1H NMR	8.14(dd, $2H_e$, J = 15.60 & J = 9.60 Hz), 8.02(d, $2H_f$, J = 10.00 Hz), 7.59(m, $4H_{c,c'}$), 7.35(t, $6H_{b,b',a}$, J = 3.60 & J = 2.80 Hz), 7.15(d, $2H_d$, J = 15.20 Hz), 3.56(s, $4H_g$), 0.98(s, $6H_h$)
	^{13}C NMR	170.65, 150.04, 134.50, 131.16, 129.13, 128.73, 124.33, 69.97, 36.69, 24.93

refined by the full-matrix least-squares method on F^2 data using SHELXTL. Tables 4–6 show the crystallographic data, selected bond distances and hydrogen bonds of $ZnLBr_2$ respectively.

2.5. Antimicrobial activity bioassay procedure

The ligand and its zinc complexes were tested for their *in vitro* antibacterial activities against Gram-negative bacteria of *E. coli* and *P. aeruginosa*; Gram-positive bacteria of *S. aureus* and *B. subtilis* and fungal strains of *C. albicans* and *Aspergillus oryzae* by disk diffusion method. For investigation into the effect of concentration, compounds were dissolved in DMSO at three different concentrations (100, 50 and 25 mg/mL). Enriched culture of the microorganisms was prepared by incubation of them in Muller–Hinton broth medium at 37 °C for 24 h. For all tests, 15 mL of sterilized Nutrient Agar as solid medium was solidified into sterilized petri plates and 0.1 mL of culture microorganism swabbed evenly on the surface of the solid medium and kept for 15 min for adsorption. Blank paper disks (6.00 mm in diameter) were saturated with a stock solution of test compounds and placed on the surface of the agar plates. All the plates were incubated at 37 °C. The growth inhibition zone around each disk as inhibitory effect was measured in millimeters after 24 h of incubation.

2.6. DNA cleavage experiments

DNA cleavage potential of the ligand and its zinc complexes has been studied by gel electrophoresis method. DNA of the *E. coli* cells was extracted using the DNA Mini Prep Extraction Kit (BIONEER, Korea) according to the manufacturer's instructions and was kept at 40 °C for the following tests. The test samples for the study of DNA cleavage potential of the compounds were prepared at a concentration of 5 mg/mL solutions in DMSO. 4 μL of each titled samples was added to 4 μL of isolated DNA in the individual microtube and incubated for 2 h at 37 °C. Extracted DNA alone as positive control and DNA treated with 30% H_2O_2 (X) as negative control were also used for monitoring the probable DNA cleavages. Then DNA containing samples were mixed with bromophenol blue dye (6 mL glycerin; 0.9 g bromophenol blue/10 mL). Finally, pure DNA, mixture of DNA and H_2O_2, ladder (1 Kb) and mixture of DNA and compound test were loaded

Table 4 Crystal data and structure refinement of $ZnLBr_2$ complex (**1**).

Chemical formula	$C_{23}H_{26}Br_2N_2Zn$
Formula weight	555.65
Crystal system	Triclinic
Crystal description	Block, colorless
Crystal size (mm)	$0.30 \times 0.16 \times 0.04$
Space group	$P\bar{1}$
Temperature (K)	296
Wavelength (Å)	0.71073
a (Å)	10.4407 (1)
b (Å)	13.9534 (1)
c (Å)	18.3360 (2)
α (°)	100.269 (1)
β (°)	93.317 (1)
γ (°)	110.775 (1)
V(Å^3)	2436.18 (4)
Z	4
D_{calc} (g cm^{-3})	1.515
μ (mm^{-1})	4.30
F(000)	1112
Absorption correction	Empirical (using intensity measurements)
Theta range for data collection (°)	1.5–30
Index ranges	$-11 \leqslant h \leqslant 11$ $-15 \leqslant k \leqslant 15$ $-20 \leqslant l \leqslant 20$
Maximum and minimum transmission	0.847 and 0.359
Refinement method	Full-matrix least-squares on F^2
Reflections collected	52150
Independent reflections	7472
Reflections with $I > 2\sigma(I)$	5782
R_{int}	0.036
Goodness-of-fit (GOF) on F^2	1.10
$R[F^2 > 2\sigma(F^2)]$	0.031
wR^a (F^2)	0.089
Data/restraints/parameters	7472/144/505
Largest difference in peak and hole (e Å^{-3})	1.07 and −0.94

[a] $w = 1/[\sigma^2(F_o^2) + (0.0417P)^2 + 1.5335P]$, where $P = (F_o^2 + 2F_c^2)/3$.

Table 5 Selected bond length (Å) and bond angle (°) data of two independent molecules of $ZnLBr_2$ complex.

Molecule 1		Molecule 2	
Bond length (Å)			
Zn1A–N1A	2.041 (3)	Zn1B–N2B	2.046 (3)
Zn1A–N2A	2.053 (3)	Zn1B–N1B	2.056 (3)
Zn1A–Br2A	2.3571 (7)	Zn1B–Br1B	2.3681 (7)
Zn1A–Br1A	2.3767 (7)	Zn1B–Br2B	2.3691 (6)
Bond angle (°)			
N1A–Zn1A–N2A	98.67 (13)	N2B–Zn1B–N1B	96.69 (12)
N1A–Zn1A–Br2A	112.35 (9)	N2B–Zn1B–Br1B	110.16 (9)
N2A–Zn1A–Br2A	106.19 (9)	N1B–Zn1B–Br1B	107.31 (9)
N1A–Zn1A–Br1A	111.68 (10)	N2B–Zn1B–Br2B	112.95 (9)
N2A–Zn1A–Br1A	112.91 (9)	N1B–Zn1B–Br2B	113.76 (9)
Br2A–Zn1A–Br1A	113.94 (2)	Br1B–Zn1B–Br2B	114.48 (3)

carefully into the wells. Electrophoresis was performed at a constant 100 V of electricity for around 30 min. Resulting bands of electrophoresis were visualized by UV light (Transilluminator, UVItec, England) and photographed.

3. Results and discussion

$ZnLX_2$ complexes were synthesized by reaction of zinc chloride, bromide and iodide salts and *N*,*N*′-bis-(3-phenyl-allylidene)-2,2-dimethyl-propane-1,3-diamine as N_2-Schiff base ligand (Fig. 1). The coordination of the ligand to the zinc ion via nitrogen donor sites were confirmed by physical and spectral data such as elemental analysis, molar conductance measurements, FT-IR, ^{1}H and ^{13}C NMR and UV–Visible. The good agreement between the experimental and theoretical data of elemental analysis (CHN) proved the ratio of 1:1 of ligand to metal salt in the complexes. Furthermore, the complex structure was confirmed by X-ray crystallography of the $ZnLBr_2$ complex. The color, melting point, yield, elemental analysis data and molar conductance values of all compounds are listed in Table 1. All compounds are stable in air and their melting points range from 93 to 247 °C. They are soluble in the dichloromethane, chloroform, DMF and DMSO. The molar conductance values of 10^{-3} M solution in DMF are in the range of 6.68–49.90 cm^2 Ω^{-1} mol^{-1} at room temperature indicating non-electrolytic behavior and stability of all compounds in solution (Halli and Sumathi, 2012; Chan et al., 2008).

3.1. IR and UV–Visible spectra

In order to clarify the mode of bonding and the effect of coordination of the ligand, IR spectra of the free ligand and its Zn(II) complexes were studied and for easy comparison have been listed in Table 2. In the free ligand spectrum, week absorptions at 3058, 3025, (2954, 2924) and (2866, 2830) cm^{-1} are assigned to the vibration stretching of aromatic, olefinic, aliphatic and iminic groups C–H respectively that smoothly shift to the lower or higher frequencies after complexation. The observation of a strong absorption at 1635 cm^{-1} in the ligand spectrum is attributed to the vibration frequency of the azomethine moieties (*ν*(C=N)). Coordination of the Schiff base to the zinc ion through the nitrogen atoms of the azomethine groups leads to the reduction of electron density in the azomethine bond and this occurrence causes a shift to lower frequencies of azomethine vibration in all the zinc complexes (Khalaji et al., 2011; Rahaman et al., 2005; Chakraborty et al., 2007). New weak absorptions in the region of 443–445 cm^{-1} in the IR spectra of complexes, are attributed to the vibration frequencies Zn–N bonds that indicates the participation of the azomethine nitrogen in coordination to zinc ion (Shebl, 2009; Anitha et al., 2012).

The electronic absorption spectra of freshly prepared DMF solution of the Schiff base and its Zn(II) complexes were recorded at room temperature and their spectral data have been tabulated as Table 2. The free Schiff base ligand shows a broad band appeared at 278 nm and it is attributed to π–π* internal electron transfer that may be due to aromatic rings, carbon–carbon and/or azomethine double bond. Coordination of ligand to metal ion via azomethine moieties leads to a shift to a longer wavenumber at 286 nm. For Zn(II) complexes with d^{10} electronic configuration, d–d electronic transition is not expected but observation of the band due to metal to ligand charge transfer (MLCT) is expectable but it is not observed in the titled compounds.

Table 6 C–H...Br and C–H...π interactions in crystal of $ZnLBr_2$ complex.

Interaction (D–H...A)		D–H (Å)	H...A (Å)	D...A (Å)	<A...H–D (°)
C–H...Br	C13B–H13B...Br1A	0.929(5)	2.982(5)	3.793(4)	146.6(2)
	C15B–H15B...Br2A	0.931(4)	2.945(5)	3.807(5)	154.5(2)
	C17B–H17B...Br2A	0.929(5)	2.852(5)	3.733(5)	158.8(3)
C–H...π	C12A–H12B...$C_g(1)$*	0.970(4)	3.112	4.051	163.12
	C12A–H12A...$C_g(2)$*	0.971(5)	3.162	4.092	161.07
	C22A–H22B...$C_g(1)$*	0.960(5)	3.269	4.122	149.00

* Ring code: $C_g(1)$: C16B, C17B, C18B, C19B, C20B, C21B; $C_g(2)$: C16A, C17A, C18A, C19A, C20A, C21A.

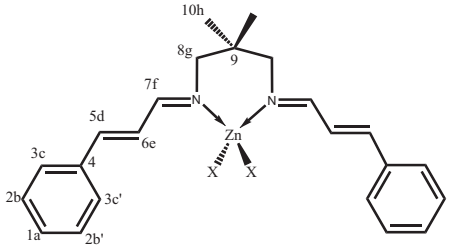

Figure 1 Structure of Zn(II) complexes X = Cl^-, Br^- and I^-.

3.2. ^1H and ^{13}C NMR spectral studies

As more evidence to confirm the structure and bonding pattern of the titled complexes, ^1H and ^{13}C NMR spectra of the ligand and its Zn(II) complexes were recorded in $CDCl_3$ solution and the data have been presented in Table 3. ^1H and ^{13}C NMR spectra data of the ligand and $ZnLX_2$ strongly support the structural formula. In the ^1H NMR spectrum of the free ligand, the doublet signal at 8.08 ppm is corresponded to the resonance of H_f (azomethine hydrogens) with $J = 7.20$ Hz due to coupling with H_e. Binding of the azomethine nitrogens to the zinc ion causes a shift to downfield regions at all zinc complex spectra (Amirnasr et al., 2002; Chohan, 2009). In the free ligand spectrum, the aromatic hydrogens of H_c, $H_{c'}$ and H_b, $H_{b'}$ and H_a appeared at 7.44 and 7.37 ppm as broad doublet and multiplet signals respectively. In the complex spectra, H_c and $H_{c'}$ appeared as a doublet of doublet signal for $ZnLCl_2$ and as a multiplet signal for $ZnLBr_2$ and $ZnLI_2$ at the region 7.59–7.70 ppm. Also in all complexes, the resonance of H_a overlapped with the signals of H_b and $H_{b'}$ and except for entry 4, in the other complexes shifted to the up field regions. In the ligand spectrum, two signals at the 7.31 and 6.93 ppm were safely assigned to ethylenic protons of H_e and H_d. After complexation, in all complexes, the resonance of H_d and H_e showed considerable shift to the upfields at 8.14–8.26 ppm as doublet of doublet signal for H_e and doublet signal for H_d. As seen in Table 3, the coupling constant for ethylenic protons is in the range of 15–16 Hz that strongly confirms trans-position of these protons around –C═C– as shown in Fig. 1. In the free ligand spectrum, H_g and H_h appeared as quartet and triplet peaks at 3.71 and 1.24 ppm due to coupling with each other. After coordination of the ligand, signals of these protons were up or down fielded.

In the ^{13}C NMR spectrum of the ligand, resonance signal of azomethine carbons (C_7, $C_{7'}$) occurred at 173.01 ppm. Good coordination of the azomethine nitrogens to zinc ion led to the observation of this signal in the upfield region at the range of 170.65–170.93 ppm. The aromatic, olefinic and aliphatic carbons signals appeared at 163.72(C_6), 138.07(C_4), 128.82(C_1), 128.53(C_3), 127.26(C_2), 126.42(C_5), 58.22(C_8), 46.25(C_9) and 18.46(C_{10}) ppm shifted to upfield or downfield ranges of 150.04–150.22(C_6), 134.46–134.50(C_4), 131.03–131.16(C_1), 129.05–129.13(C_3), 128.69–128.73(C_2), 124.23–124.33(C_5), 69.97–71.84(C_8), 36.69–36.91(C_9) and 24.53–24.93(C_{10}) ppm. These signals and their shifts in complexes as compared with free ligand are in good agreement with the structure of zinc halide complexes.

3.3. Crystal structure

The $ZnLBr_2$ complex structure has been identified by single crystal X-ray analysis. The ORTEP view of the complex is

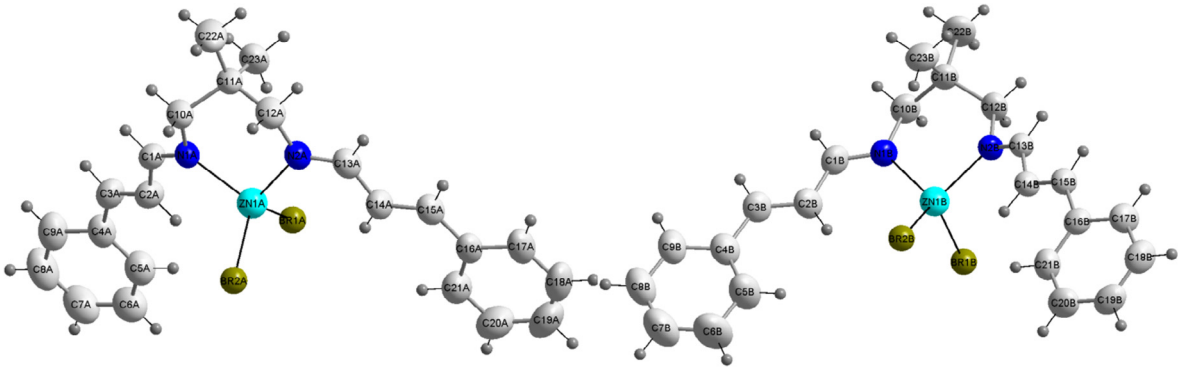

Figure 2 ORTEP diagram of complex **1** with the atom numbering scheme. Atoms are represented by 25% probability thermal ellipsoids. Hydrogen atoms are omitted for clarity.

shown in Fig. 2. Crystallographic data and refinement have been tabulated as Table 4. Some selected bond lengths and angles are given in Table 5. The complex crystallizes in a triclinic system with the space group of $P\bar{1}$, with two crystallographically independent molecules noted as A and B per asymmetric unit cell (Fig. 3). The crystal structure of the complex reveals the presence of a structure consisting of a bidentate N_2-donor Schiff base, two bromide anions and a zinc(II) ion in the discrete monomeric species. Both Zn1A and Zn1B are almost in slightly distorted tetrahedral environments ($\tau_4 = 0.94$ for Zn1A and $\tau_4 = 0.93$ for Zn1B whereas $\tau_4 = 0$ and $\tau_4 = 1$ are attributed to square planar geometry and tetrahedral geometry respectively) (Yang et al., 2007).

The average bond lengths of Zn–Br (2.37 Å in both molecules) and Zn–N (2.05 Å in both molecules) well agreed with the Zn–Br and Zn–N bond lengths in other reported tetrahedral zinc complexes, such as [Zn(nca$_2$en)Br$_2$] (2.35 Å for Zn–Br and 2.05 Å for Zn–N) and [Zn(Salen)Br$_2$] (2.35 Å for Zn–Br and 2.08 Å for Zn–N) (Dehghanpour and Mahmoudi, 2007; Taylor et al., 2006). It is to be noted that Zn–N bond distances in the current structure are considerably shorter than some Zn–N distances reported for some organo-zinc structures (2.156-2.410 Å) (Melnik et al., 1995; Jastrzebski et al., 2006). The angle values around the zinc center [N–Zn–Br: 106.19–113.76°; N–Zn–N: 96.69 and 98.67°; Br–Zn–Br: 113.94 and 114.48°] are in good agreement with other ZnN_2Br_2 tetrahedral complexes

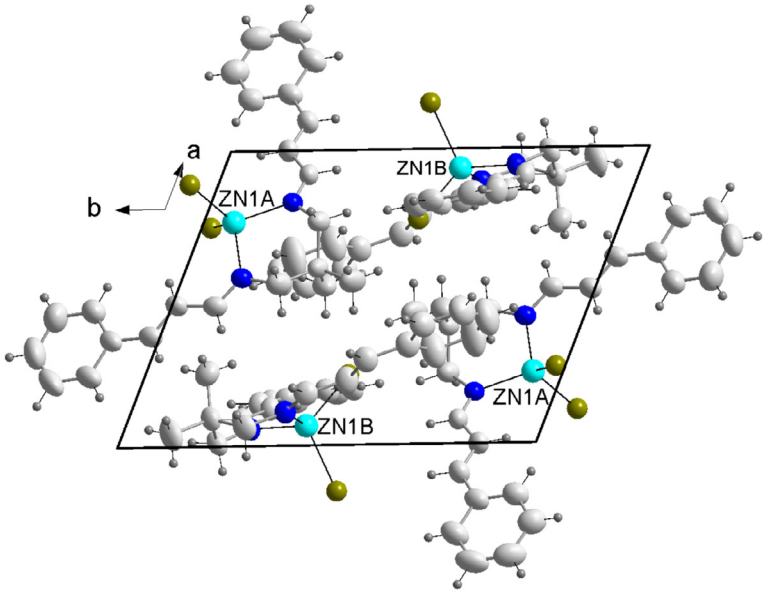

Figure 3 Unit cell structure of ZnLBr$_2$ complex indicating two molecules with different symmetry equivalence in the asymmetric unit.

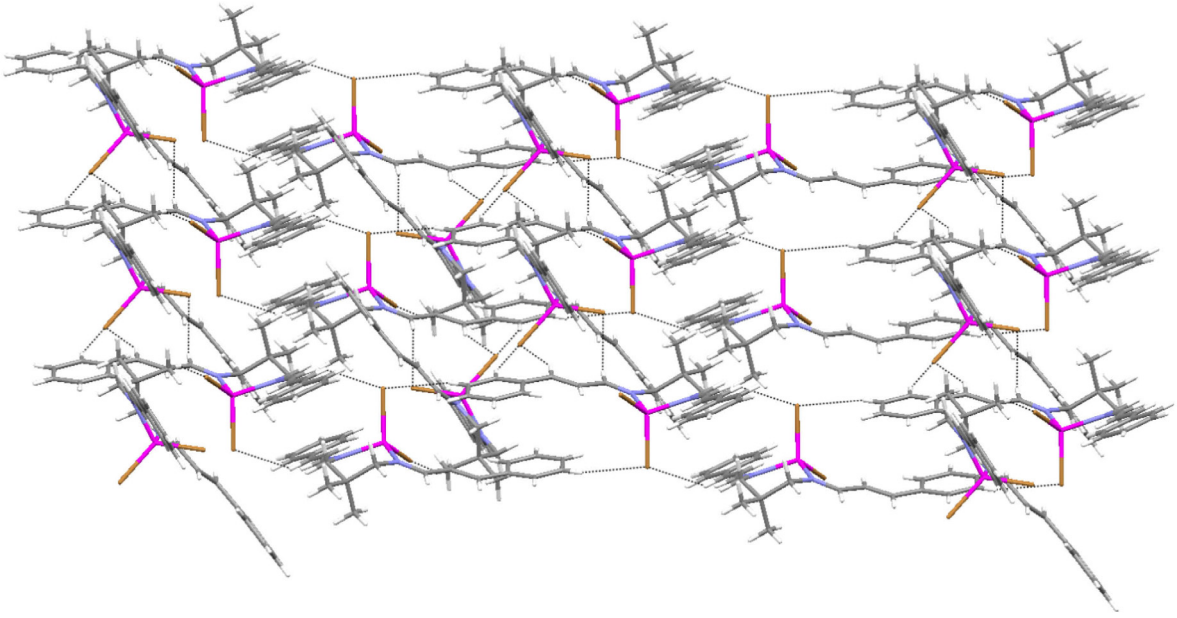

Figure 4 Aggregation of ZnLBr$_2$ compound via C–H...Br interactions.

(Dehghanpour and Mahmoudi, 2007; Taylor et al., 2006; Khalaji et al., 2010). The N–Zn–N and Br–Zn–Br bond angles are respectively smaller and larger than the ideal tetrahedral values. Of course, the angle value of N–Zn–N (96.69 and 98.67°) in the current structure is smaller than that in $[Zn(CH_2)_3NMe_2))_2]$ (109.7°) while is larger than that in $[Zn(Me_4en)C_5H_7)Cl]$ (84.5°) that each two mentioned complexes contain non-Schiff base chelating ligands (Melnik et al., 1995). In the Zn1A molecule, the aromatic rings of the ligand (L) are almost coplanar with the dihedral angle of 6.63°, and the dihedral angle between the

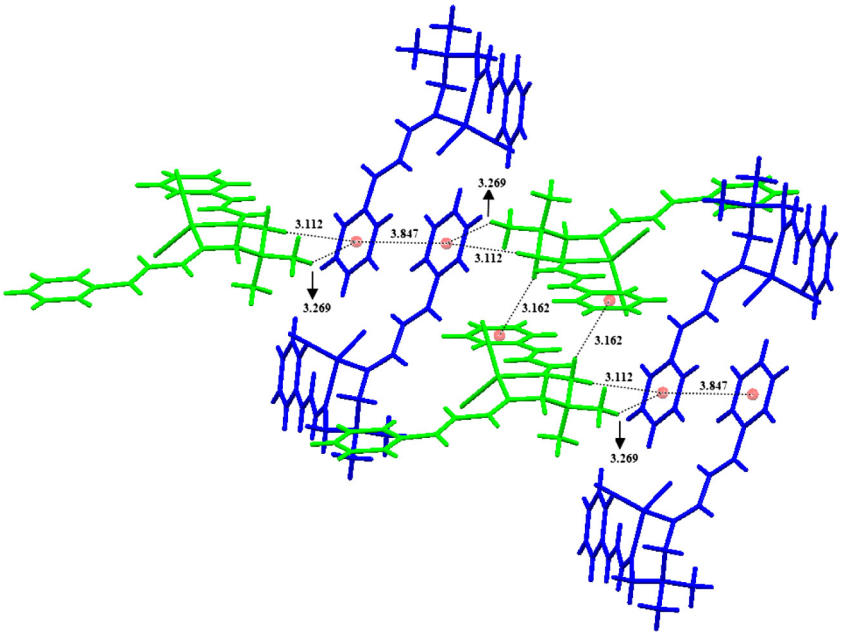

Figure 5 π–π and C–H...π interactions in $ZnLBr_2$ complex (green: Zn1A molecule; blue: Zn1B molecule).

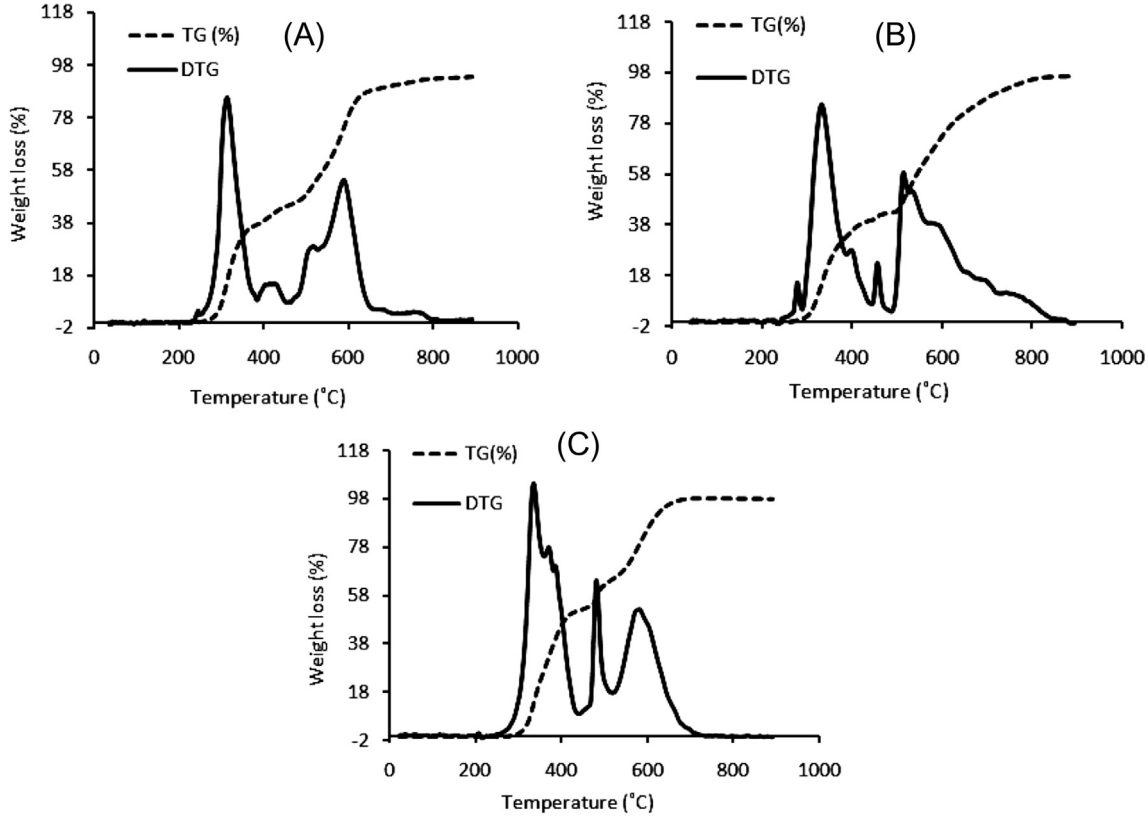

Figure 6 TG/DTG plots of (A) $ZnLCl_2$, (B) $ZnLBr_2$ and (C) $ZnLI_2$.

aromatic rings of the ligand (L) in Zn1B molecule is 21.04°. Detailed structural analysis shows that there are three non-classical hydrogen bonding C–H...Br (C13B–H13B...Br1A = 2.98 Å; C15B–H15B...Br2A = 2.95 Å; C17B–H17B...Br2A = 2.85 Å) between the discrete molecules in the structure (Table 6). These interactions, which are in the expected ranges (Horn et al., 2003; Steiner, 2002), connect the molecules together forming a three dimensional network (Fig. 4). Also the analysis of π–π and C–H...π interactions in this complex shows that the π–π interaction between the phenyl rings of the adjacent Zn1B molecules (Fig. 5) was 3.847 Å and an inter-planar atom–atom distance was 3.471 Å between the parallel stacking pairs with a dihedral angle of 0.0°. Several C–H...π interactions exist in the packing structure of the $ZnLBr_2$ complex (Fig. 5). The most significant interactions of these types are listed in Table 6. Distances and angles are well placed within the accepted range of C–H...π interactions (Nishio et al., 1998). These interactions play an important role for stabilizing the molecular structure and give rise to a 3D supramolecular structure.

3.4. Thermal analysis (TG/DTG) of complexes

Investigation into thermal stability and existence of any water in the coordination sphere of the complexes has been performed at a heating rate of 10 °C/min under nitrogen atmosphere in the range from room temperature up to 1000 °C. As seen in Fig. 6, thermo-grams of all complexes did not show any weight loss up to 200 °C confirming the absence of any lattice or coordinated water molecules. Regarding TG/DTG plots of all complexes, it was found that $ZnLCl_2$ and $ZnLI_2$ complexes were decomposed via four thermal steps while the degradation of $ZnLBr_2$ occurred via about seven thermal steps. It is to be noted that the final steps are very near to each other so that they are distinguishable only based on DTG plot changes. Resulting data of these thermal steps including temperature range, mass loss (%) and thermo-kinetic activation parameters for each decomposition step have been listed in Table 7. The suggested lost segments at each decomposition step for all complexes have also been found in Table 7. As mentioned in Table 7, at the end of decomposition process, the complexes lose 88.22–98.40% of their total mass and finally leave out zinc metal as residue. As a typical model, the suggested decomposition pathway for the zinc chloride complex is illustrated in Fig. 7. This complex loses the segments of $C_{13}H_{11}$, C_3H_3, C_3H_5 and $C_4H_7Cl_2N_2$, via steps 1–4 respectively and some zinc metal residue remained in the final. In continuation of the thermal investigation, Arrhenius constant (A), activation energy (E^*), enthalpy (ΔH^*), entropy (ΔS^*) and Gibbs free energy (ΔG^*) of the decomposition process for each thermal step have been evaluated by using TG/DTG plots and Coats–Redfern relationship (Coats and Redfern, 1964). The positive values of activation energies (E^*) evaluated in the range of 34.41–158.61 kJ mol^{-1} for the thermal decomposition steps is an evidence of the thermal stability of the complexes. In all decomposition stages ΔH^* and ΔG^* values were found positive in the range of

Table 7 Thermal decomposition steps, mass loss (%), proposed lost segments, final residue thermo-kinetic activation parameters of each decomposition step for zinc complexes.

Compound	Temperature step (°C)	~Mass loss (%)	Proposed segment	Total Mass loss (%)	Final residue	E^* (kJ mol^{-1})	A (s^{-1})	ΔS^* (kJ mol^{-1} K^{-1})	ΔH^* (kJ mol^{-1})	ΔG^* (kJ mol^{-1})
$ZnLCl_2$	200–385	37.33	$C_{13}H_{11}$	88.22	Zn	158.61	2.53×10^{12}	-1.31×10^{1}	153.73	1.61×10^{2}
	385–465	7.65	C_3H_3			34.41	9.19×10^{-1}	-2.53×10^{2}	28.69	2.02×10^{2}
	465–532	10.88	C_3H_5			116.99	2.90×10^{5}	-1.48×10^{2}	110.41	2.28×10^{2}
	532–655	43.24	$C_4H_7Cl_2N_2$			86.91	4.19×10^{2}	-2.04×10^{2}	79.73	2.55×10^{2}
$ZnLBr_2$	200–290	1.41	CH	96.92	Zn	441.34	6.55×10^{39}	5.12×10^{2}	436.76	1.55×10^{2}
	290–386	32.28	$C_{13}H_{11}$			140.67	2.64×10^{9}	-7.04×10^{1}	135.65	1.78×10^{2}
	386–440	6.42	C_3H_3			57.86	9.89×10^{1}	-2.13×10^{2}	52.29	1.95×10^{2}
	400–485	3.00	CH			83.58	5.20×10^{3}	-1.81×10^{2}	77.52	2.09×10^{2}
	485–568	22.45	C_3H_6Br			66.17	3.91×10^{1}	-2.23×10^{2}	59.64	2.34×10^{2}
	568–730	25.62	$C_2H_4BrN_2$			35.04	1.37×10^{-1}	-2.70×10^{2}	27.99	2.57×10^{2}
	730–870	5.74	$Zn_{0.5}$			27.99	4.93×10^{-2}	-2.80×10^{2}	19.56	3.04×10^{2}
$ZnLI_2$	200–360	27.48	$C_{14}H_{12}$	98.40	Zn	220.38	2.99×10^{16}	6.46×10^{1}	215.33	1.76×10^{2}
	360–440	24.56	$C_9H_{14}N_2$			80.07	6.12×10^{3}	-1.79×10^{2}	74.72	1.90×10^{2}
	440–520	12.93	$I_{0.65}$			75.10	5.04×10^{2}	-2.01×10^{2}	68.82	2.20×10^{2}
	520–720	33.43	$I_{1.35}Zn_{0.70}$			51.77	2.06	-2.48×10^{2}	44.67	2.56×10^{2}

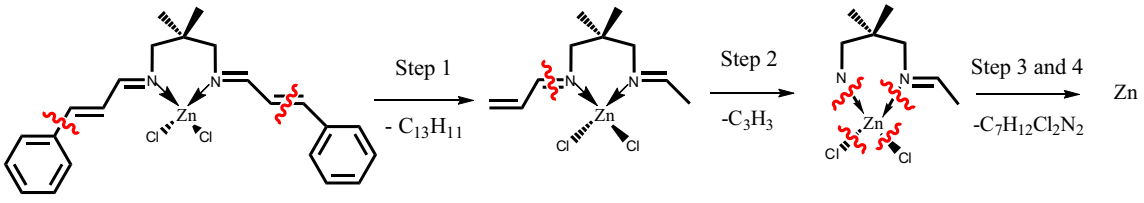

Figure 7 Proposed decomposition pathway of zinc chloride complex.

28.69–153.73 kJ mol^{-1} for ΔH^* and 161–256 kJ mol^{-1} for ΔG^* reflecting endothermic character of decomposition processes. In most of the thermal decomposition steps, negative values in the range of −3.1 to −267 kJ mol^{-1} K^{-1} were obtained for entropy of activation (ΔS^*). These negative values indicate that the processes are slower than the normal decomposition reactions or suggest that the thermally activated compounds have a more ordered or more rigid structure than that of the not-decomposed compounds/fragments (Vinodkumar et al., 2000; Ismail et al., 2012).

3.5. Antibacterial and anti-fungal activity

Schiff base ligand and zinc(II) complexes were screened *in vitro* for their abilities as antibacterial and antifungal activities against *E. coli* and *P. aeruginosa* as Gram-negative; *S. aureus* and *B. subtilis* as Gram-positive bacteria and *against C. albicans* and *A. oryzae* as fungal strains. Antibacterial and antifungal activities as the zones of inhibition for all compounds are tabulated as Tables 8 and 9. Resulting data of these investigations revealed that the inhibitory effect is susceptible to the concentration of the compound used for inhibition so that the activity is greatly enhanced at the higher concentration of compound. In case of antibacterial activity, the $ZnLI_2$ complex was found highly effective against *E. coli*, *S. aureus* and *B. subtilis* in the following order *B. subtilis* > *S. aureus* > *B. subtilis* while against *P. aeruginosa*, $ZnLCl_2$ showed better antibacterial activity. Antifungal study of zinc complexes exhibited good activity against *C. albicans* and *Aspergillus niger* than the free ligand. The growth inhibitory effect of complexes against *A. niger* was found better than against *C. albicans*. The zinc bromide complex demonstrated the highest zone of inhibition in three concentrations against *A. oryzae* while zinc iodide complex showed the highest zone of inhibition against *C. albicans*.

In general, the activity of Schiff bases may be due to the chelating properties of the azomethine group used in metal transport across the bacterial membranes or in attaching to a specific site of the bacterial cells from which it can interfere with their growth (Rehman et al., 2008; Amin et al., 2010). Coordination of ligand to the metal ion makes the ligand a stronger antibacterial agent so that the zinc complexes show increased antibacterial and antifungal activity than the free ligand. This enhanced activity may be due to electron delocalization over the whole chelate ring upon complexation. Such chelation increases lipophilicity and enhances permeation through the lipid layer of the cell membrane (chelation theory) (Singh et al., 2009; Angelusiu et al., 2010).

3.6. DNA cleavage efficiency

Interactions between Zn (II) complexes and DNA were investigated by the cleavage assay of plasmid DNA ($pMalC_2X$ DNA of *E. Coli*). The ability of compounds to cleavage plasmid DNA was analyzed by monitoring the conversion of supercoiled circular DNA (Form I) to nicked (Form II) and the linear (Form III) form of DNA. The amounts of strand scission were assessed by agarose gel electrophoresis. During electrophoresis, depending on the rate of migration, three forms of DNA are separated. The compact Form I migrates relatively fast while the nicked Form II migrates slowly, and the linearized form (Form III) migrates between Forms I and II. These changes are clearly observed in the gel electrophoresis by the change or disappearance of the intensity of the supercoiled band and appearance of new bands or smear in gel diagram (Fig. 8). In this figure L, X and C are attributed

Table 8 Bactericidal screening data (zone of inhibition (mm)) of ligand and its Zn(II) complexes at three concentrations (mg/mL).

Compound	Diameter of inhibition zone (mm)											
	Gram negative bacteria						Gram positive bacteria					
	Escherichia coli			*P. aeruginosa*			*Bacillus subtilis*			*Staphylococcus aureus*		
	100 (mg/mL)	50 (mg/mL)	25 (mg/mL)	100 (mg/mL)	50 (mg/mL)	25 (mg/mL)	100 (mg/mL)	50 (mg/mL)	25 (mg/mL)	100 (mg/mL)	50 (mg/mL)	25 (mg/mL)
Ligand	8.60	7.35	7.20	11.60	11.30	9.98	14.36	11.20	7.65	8.52	6.68	6.30
$ZnLCl_2$	10.58	9.38	8.30	13.56	11.00	9.01	14.50	12.48	11.50	14.58	12.50	9.00
$ZnLBr_2$	14.00	12.50	10.44	11.50	9.35	8.00	16.64	14.60	12.5	17.70	14.00	10.00
$ZnLI_2$	16.70	14.50	12.48	10.45	10.00	9.30	22.00	19.70	13.56	19.67	15.70	15.00

Table 9 Antifungal activities of constructed disks (soaked in 100, 50 and 25 mg/mL of Schiff base and its zinc complexes) based on diameter zone (mm) against various funguses.

Compound	Diameter of inhibition zone (mm)					
	Fungous					
	C. albicans			*Aspergillus oryzae*		
	100 (mg/mL)	50 (mg/mL)	25 (mg/mL)	100 (mg/mL)	50 (mg/mL)	25 (mg/mL)
Ligand	16.40	11.72	11.31	15.30	14.10	11.90
$ZnLCl_2$	19.30	17.00	15.65	23.15	18.17	14.00
$ZnLBr_2$	20.00	17.30	15.00	31.30	29.00	17.70
$ZnLI_2$	20.45	18.00	16.3	29.00	17.75	9.00

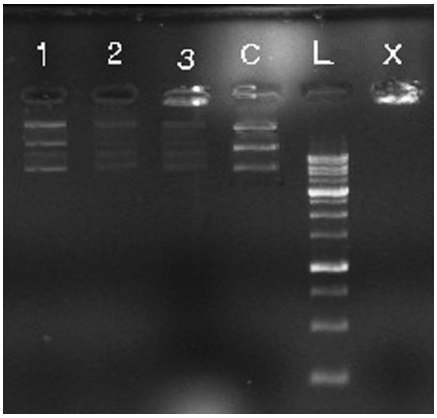

Figure 8 Agarose gel electrophoresis photograph for DNA cleavage study of Zn(II) complexes. Lane L = ladder, Lane X = DNA + H_2O_2, Lane C = control DNA. Lane 1 = DNA + $ZnLCl_2$, Lane 2 = DNA + $ZnLBr_2$ and Lane 3 = DNA + $ZnLI_2$.

to the ladder, mixture of DNA and H_2O_2 and control DNA respectively. Lanes 1 to 3 are attributed to $ZnLCl_2$, $ZnLBr_2$ and $ZnLI_2$ mixed with DNA respectively. As illustrated in Fig. 8, a difference was observed in the bands of $ZnLBr_2$ and $ZnLI_2$ complexes (lanes 2 and 3) as compared to those of the control DNA showing the partial cleavage of DNA but for $ZnLCl_2$ (lane 1) any apparent cleavage of DNA is observed. The presence of a smear in the gel diagram indicates that the mechanism may involve radical cleavage (Kaczmarek et al., 2009; Refat et al., 2009; Zhang and Lippard, 2003). DNA cleavage potential of the compounds may suggest that the compound inhibits the growth of pathogenic organisms by cleavage of their genome.

4. Conclusion

In this work, synthesis and characterization of three new four coordinated zinc(II) complexes have been reported. Elemental analyses of complexes suggested the general formula of $ZnLX_2$ for all complexes. Low molar conductivities in DMF indicated non-electrolyte character of all complexes. Spectral data were in good agreement with the coordination of ligand via azomethine nitrogens to the zinc ion. The $ZnLBr_2$ complex was subjected to X-ray single crystal analysis for confirmation of complex structure. The complex crystallized as twin in the triclinic system with a space group of $P\bar{1}$. The zinc bromide complex showed a perfect tetrahedral environment around the zinc ion. Detailed structural analysis showed the existence of three non-classical hydrogen bondings of C–H...Br in the structure. Various C–H...π and C–H...Br in the molecular structure then causes a 3D supramolecular structure of the $ZnLBr_2$ complex. A biological investigation showed that the Schiff base and its complexes are antibacterial/antifungal active against Gram-negative bacteria; *E. coli* and *P. aeruginosa* and Gram-positive bacteria *S. aureus* and *B. subtilis)* and antifungal (*A. oryzae* and *C. albicans*). Also the ability of the complexes for DNA cleavage was studied by agarose gel electrophoresis method. Finally, thermal behavior of the complexes has been investigated by thermo-gravimetric method and then some activation kinetics parameters of decomposition steps were evaluated.

Acknowledgement

Partial support of this work by Yasouj University is acknowledged. Also X-ray record by University of Waterloo is appreciated.

Appendix A. Supplementary data

Supplementary data associated with this article can be found, in the online version, at http://dx.doi.org/10.1016/j.arabjc.2014.11.005. CCDC 1006629 contains the supplementary crystallographic data for this paper. These data can be obtained free of charge via http://www.ccdc.cam.ac.uk/conts/retrieving.html (or from the Cambridge Crystallographic Data Centre, 12, Union Road, Cambridge CB2 1EZ, UK; fax: +44 1223 336033).

References

Abdel Aziz, A.A., Badr, I.H.A., El-Sayed, I.S.A., 2012. Synthesis, spectroscopic, photoluminescence properties and biological evaluation of novel Zn(II) and Al(III) complexes of NOON tetradentate Schiff bases. Spectrochim. Acta A 97, 388–396.

Amin, R., Krammer, B., Abdel-Kader, N., Verwanger, T., El-Ansary, A., 2010. Antibacterial effect of some benzopyrone derivatives. Eur. J. Med. Chem. 45, 372–378.

Amirnasr, M., Mahmoudkhani, A.H., Gorji, A., Dehghanpour, S., Bijanzadeh, H.R., 2002. Cobalt(II), nickel(II), and zinc(II) complexes with bidentate *N*,*N*′-bis(β-phenylcinnamaldehyde)-1,2-diiminoethane Schiff base: synthesis and structures. Polyhedron 21, 2733–2742.

Angelusiu, M.V., Barbuceanu, S.F., Draghici, C., Almajan, G.L., 2010. New Cu(II), Co(II), Ni(II) complexes with aroyl-hydrazone based ligand. Synthesis, spectroscopic characterization and in vitro antibacterial evaluation. Eur. J. Med. Chem. 45, 2055–2062.

Anitha, C., Sheela, C.D., Tharmaraj, P., Sumathi, S., 2012. Synthesis and characterization of VO(II), Co(II), Ni(II), Cu(II) and Zn(II) complexes of chromone based azo-linked Schiff base ligand. Spectrochim. Acta A 96, 493–500.

Arjmand, F., Sayeed, F., Muddassir, M., 2011. Synthesis of new chiral heterocyclic Schiff base modulated Cu(II)/Zn(II) complexes: their comparative binding studies with CT-DNA, mononucleotides and cleavage activity. J. Photochem. Photobiol., B 103, 166–179.

Chakraborty, J., Thakurt, S., Samanta, B., Ray, A., Pilet, G., Batten, S.R., Jensen, P., Mitra, S., 2007. Synthesis, characterization and crystal structures of three trinuclear cadmium(II) complexes with multidentate Schiff base ligands. Polyhedron 26, 5139–5149.

Chan, M.E., Crouse, K.A., Tahir, M.I.M., Rosli, R., Umar-Tsafe, N., Cowley, A.R., 2008. Synthesis and characterization of cobalt (II), nickel (II), copper (II), zinc (II) and cadmium (II) complexes of benzyl-1-(thiophen-2-yl) ethylidene] hydrazine carbodithioate and benzyl-[1-(thiophen-3-yl) ethylidene] hydrazine carbodithioate and the X-ray crystal structure of bis benzyl-[1-(thiophen-2-yl) ethylidene] hydrazine carbodithioate nickel (II). Polyhedron 27, 1141–1149.

Chohan, Z.H., 2009. Antibacterial dimeric copper(II) complexes with chromone-derived compounds. Trans. Met. Chem. 34, 153–161.

Coats, A.W., Redfern, J.P., 1964. Kinetic parameters from thermogravimetric data. Nature 201, 68–69.

Dehghanpour, S., Mahmoudi, A., 2007. Synthesis and characterization of cobalt(II), nickel(II), and zinc(II) complexes with *N*,*N*′-bis(2-nitrocinnamaldehyde)-1,2-diiminoethane ligand. Crystal structure of Zn(nca2en)Br2. Synth. React. Inorg. Met. Org. Nano-Met. Chem. 37, 35–40.

El-Sherif, A.A., Eldebss, T.M.A., 2011. Synthesis, spectral characterization, solution equilibria, in vitro antibacterial and cytotoxic

activities of Cu(II), Ni(II), Mn(II), Co(II) and Zn(II) complexes with schiff base derived from 5-bromosalicylaldehyde and 2-aminomethylthiophene. Spectrochim. Acta A 79, 1803–1814.

Halli, M.B., Sumathi, R.B., 2012. Synthesis, spectroscopic, antimicrobial and DNA cleavage studies of new Co(II), Ni(II), Cu(II), Cd(II), Zn(II) and Hg(II) complexes with naphthofuran-2-carbohydrazide Schiff base. J. Mol. Struct. 1022, 130–138.

Harinath, Y., Kumar Reddy, D.H., Kumar, B.N., Apparao, Ch., Seshaiah, K., 2013. Synthesis, spectral characterization and antioxidant activity studies of a bidentate Schiff base, 5-methyl thiophene-2-carboxaldehyde-carbohydrazone and its Cd(II), Cu(II), Ni(II) and Zn(II) complexes. Spectrochim. Acta A 101, 264–272.

Horn, C.J., Blake, A.J., Champness, N.R., Garau, A., Lippolis, V., Wilson, C., Schroder, M., 2003. Helical templating of polyiodide networks at a binuclear metallo complex. Chem. Commun., 312–313.

Ismail, T.M.A., Saleh, A.A., El Ghamry, M.A., 2012. Tetra- and hexadentate Schiff base ligands and their Ni(II), Cu(II) and Zn(II) complexes. Synthesis, spectral, magnetic and thermal studies. Spectrochim. Acta A 86, 276–288.

Jastrzebski, J.T.B.H., Boersma, J., Van Koten, G., 2006. In: Rappoport, Z., Marek, I. (Eds.), Patai Series: The Chemistry of Functional Groups, the Chemistry of Organozinc Compounds, Part 1. Wiley, Chichester, pp. 31–135.

Joohari, S., 2013. Synthesis and identification of some new cadmium(ii) halide complexes. Inorg. Chem. Indian J. 8, 123–127.

Kaczmarek, M.T., Jastrzab, R., Kedzia, E.H., Paryzek,, W.R., 2009. Self-assembled synthesis, characterization and antimicrobial activity of zinc(II) salicylaldimine complexes. Inorg. Chim. Acta 362, 3127–3133.

Khalaji, A.D., Weil, M., Grivani, G., Akerdi, S.J., 2010. Synthesis, characterization, and crystal structure of two zinc(II) halide complexes with the symmetrical bidentate Schiff-base ligand (3,4-MeO-ba)2en. Monatsh. Chem. 141, 539–543.

Khalaji, A.D., Grivani, G., Rezaei, M., Fejfarova, K., Dusek, M., 2011. Synthesis and spectral characterization of mercury(II) complexes with the bidentate Schiff base ligand *N*,*N*′-bis(2,3-dimethoxybenzylidene)-1,2-diaminoethane: The crystal structures of [Hg((23-MeO-ba)2en)I2] and [Hg((23-MeO-ba)2en)Br 2]. Polyhedron 30, 2790–2794.

Kowol, C.R., Trondl, R., Arion, V.B., Jakupec, M.A., Lichtscheidl, I., Keppler, B.K., 2010. Fluorescence properties and cellular distribution of the investigational anticancer drug Triapine (3-aminopyridine-2-carboxaldehyde thiosemicarbazone) and its zinc(II) complex. J. Chem. Soc. Dalton Trans. 39, 704–706.

Melnik, M., Skorepa, J., Gyiiryovi, K., Holloway, C.E., 1995. Structural analyses of organozinc compounds. J. Organomet. Chem. 503, 1–9.

Montazerozohori, M., Yadegari, S., Naghiha, A., Veyseh, S., 2013. Synthesis, characterization, electrochemical behavior, thermal study and antibacterial/antifungal properties of some new zinc(II) coordination compounds. J. Ind. Eng. Chem. 20, 118–126.

Montazerozohori, M., Musavi, S.A., Naghiha, A., Montazer Zohour, M., 2014a. Some new nano-structure zinc(II) coordination compounds of an imidazolidine Schiff base: spectral, thermal, antimicrobial properties and DNA interaction. Spectrochim. Acta A 129, 382–391.

Montazerozohori, M., Musavi, S.A., Naghiha, A., Veyseh, S., 2014b. Some new IIB group complexes of an imidazolidine ligand: Synthesis, spectral characterization, electrochemical, thermal and antimicrobial properties. J. Chem. Sci. 126, 227–238.

Montazerozohori, M., Zahedi, S., Naghiha, A., Montazer Zohour, M., 2014c. Synthesis, characterization and thermal behavior of antibacterial and antifungal active zinc complexes of bis (3(4-dimethylaminophenyl)-allylidene-1,2-diaminoethane. Mater. Sci. Eng., C 35, 195–204.

Nishio, M., Hirota, M., Umezawa, Y., 1998. In: Marchand, A.P. (Ed.), Methods in Stereochemical Analysis. Wiley–VCH, New York, pp. 19–33.

Nitha, L.P., Aswathy, R., Mathews, N.E., kumari, B.S., Mohanan, K., 2014. Synthesis, spectroscopic characterization, DNA cleavage, superoxidase dismutase activity and antibacterial properties of some transition metal complexes of a novel bidentate Schiff base derived from isatin and 2-aminopyrimidine. Spectrochim. Acta A 118, 154–161.

Rahaman, S.H., Ghosh, R., Lu, T.-H., Ghosh, B.K., 2005. Chelating *N*,*N*′-(bis(pyridin-2-yl)alkylidene)propane-1,3-diamine pseudohalide copper(II) and cadmium(II) coordination compounds: Synthesis, structure and luminescence properties of [M(bpap)(X)]ClO4 and [M(bpap)(X)2] [M = Cu, Cd; image, NCS−]. Polyhedron 24, 1525–1532.

Refat, M.S., El-Deen, I.M., Anwer, Z.M., El-Ghol, S., 2009. Spectroscopic, antibacterial activity and thermogravimetric studies. J. Mol. Struct. 920, 149–162.

Rehman, W., Baloch, M.K., Badshah, A., 2008. Synthesis, spectral characterization and bio-analysis of some organotin(IV) complexes. Eur. J. Med. Chem. 43, 2380–2385.

Rosu, T., Pahontu, E., Pasculescu, S., Georgescu, R., Stanica, N., Curaj, A., Popescu, A., Leabu, M., 2010. Synthesis and characterization of novel Cu(II) and Pd(II) complexes with 2-hydroxy-8-R-tricyclo[7.3.1.0.2,7]tridecane-13-one thiosemicarbazone. Study on biological activity. Eur. J. Med. Chem. 45, 1627–1634.

Shebl, M., 2009. Synthesis, spectral and magnetic studies of mono- and bi-nuclear metal complexes of a new bis(tridentate NO2) Schiff base ligand derived from 4,6-diacetylresorcinol and ethanolamine. Spectrochim. Acta A 73, 313–323.

Singh, R.V., Chaudhary, P., Chauhan, S., Swami, M., 2009. Microwave-assisted synthesis, characterization and biological activities of organotin (IV) complexes with some thio Schiff bases. Spectrochim. Acta A 72, 260–268.

Steiner, T., 2002. The hydrogen bond in the solid state. Angew. Chem. Int. Ed. 41 (2002), 48–76.

Taylor, M.K., Stevenson, D.E., Berlouis, L.E.A., Kennedy, A.R., Reglinski, J., 2006. Modelling the impact of geometric parameters on the redox potential of blue copper proteins. J. Inorg. Biochem. 100, 250–259.

Vinodkumar, C.R., Muraleedharan Nair, M.K., Radhakrishnan, P.K., 2000. Thermal studies on lanthanide nitrate complexes. Therm. Anal. Cal. 61, 143–149.

Yang, L., Powell, D.R., Houser, R.P., 2007. Structural variation in copper(I) complexes with pyridylmethylamide ligands: structural analysis with a new four-coordinate geometry index, τ4. Dalton Trans., 955–964.

You, Z.L., Ni, L.L., Shi, D.H., Bai, S., 2010. Synthesis, structures, and urease inhibitory activities of three copper(II) and zinc(II) complexes with 2-{[2-(2-hydroxyethylamino)ethylimino]methyl}-4-nitrophenol. Eur. J. Med. Chem. 45, 3196–3199.

Zhang, C.X., Lippard, S.J., 2003. New metal complexes as potential therapeutics. Curr. Opin. Chem. Biol. 7, 481–489.

Zhang, N., Fan, Y., Zhang, Z., Zuo, J., Zhang, P., Wang, Q., Liu, S., Bi, C., 2012. Synthesis, crystal structures, and magnetic properties of trinuclear cobalt(II) and nickel(II) complexes with oxamido vanadium(IV)-oxo complex ligand. Inorg. Chem. Commun. 22, 68–72.